Creep behaviour of eco-friendly sandwich composite materials under hygrothermal conditions

Authors: Benjamin Sala[*1], Ponnapat Watjanatepin[2], Hanie Zarafshani[2], Violaine Guicheret-Retel[1], Frédérique Trivaudey[1], Fabrizio Scarpa[3], Karel Van Acker[4], Vincent Placet[1]

Affiliation: [1]Univ. Bourgogne Franche-Comté, FEMTO-ST Institute, Department of Applied Mechanics, F-25000 Besançon.

[2]Department of Materials Engineering, KU Leuven, Kasteelpark Arenberg 44, 3001, Leuven, Belgium

[3]Bristol Composites Institute, University of Bristol, BS8 1 T, UKR, Bristol, UK

[4]Center for Economics and Corporate Sustainability (CEDON), KU Leuven, Warmoesberg 26, BE-1000 Brussels, Belgium

Abstract:

This work describes a new class of sandwich panels made of hemp fibre composites and eco-friendly core materials (balsa, paper honeycomb and recycled PET foam). The biobased panels are designed to replace analogous glass fibre mat solutions widespread in the automotive sector. Compared to their fossil benchmark, these panels show a significant reduction in terms of Global Warming Potential (from 29 to 40%). Moreover, creep/recovery tests performed under two different hygrothermal environments (23°C-50% RH and 70°C-65% RH) suggest that the time-delayed behaviour has to be considered in the design of the bio-based sandwich panels, particularly when exposed to severe environments.

Keywords: sandwich composite, creep/recovery, hygrothermal environment, LCA

1. INTRODUCTION

Sandwich composite structures were first used in airframes during World War I [1] and their first mass production took place then in the United Kingdom during World War II [2]. Nowadays, the use of these materials is not limited to the aeronautical sector. Sandwich structures are also used in ground transportation, for rail and road vehicles [1,3], as well as in civil engineering (bridge decks), shipbuilding and the sailing industry (sailboat hulls),

and within the energy sector (wind turbine blades) [1,4,5]. During the last ten years, environmental concerns, societal and regulatory pressures have pushed several industries to reduce their ecological footprint and greenhouse gas emissions, and also to develop more eco-friendly materials. Sandwich composite structures made of bio-based materials such as plant fibre composites (PFCs) provide alternative solutions to replace traditional glass fibre composite sandwich structures [6]. The use of natural fibres leads to a reduction of greenhouse gases and pollutant emissions, and contributes to a lower environmental impact of non-renewable energy and fossil-based materials, together with better bio-degradability properties in the End-of-Life phases of the products. A review by Weiss et al. [7] about over 40 life cycle assessment (LCA) studies on 60 different bio-based materials indicates that on average, one ton of bio-derived materials can help reducing the primary energy consumption by 55 ± 34 GJ, when compared with one ton of fossil-derived materials; this leads to a significant reduction in terms of carbon footprint. Bio-derived products can also increase the impact of the related agricultural activities, such as land use and eutrophication, among others [8]. Le Duigou et al. [6] have also demonstrated that flax fibre-reinforced polylactic acid (PLA) composites can have a lower environmental impact when compared to their conventional glass fibre-reinforced polyester composite counterparts. A recent review by Malviya et al. [9] has also re-iterated the potential of the overall environmental sustainability of natural fibre composites when compared to their fossil fibre composites counterparts, especially in terms of greenhouse gas emission reductions. This feature can be in particular explained by the lack (or minimal release) of new stored carbon emissions from the biomass from which plant fibres are sourced; this is not the case of petroleum-based reinforcements [10]. Furthermore, the cultivation of biomass also affects the temporary carbon sequestration during its growth cycle [11]. To this end, different LCA studies of plant fibre-reinforced composites have demonstrated a lower carbon footprint than their synthetic counterparts [12–14]. However, to date, the use of bio-based sandwich panels in structural or semi-structural applications is mainly limited to demonstrators and prototypes, and has not yet reached the stage of mass production. Faurecia has developed a sandwich composite panel with flax fibre skins and a cardboard honeycomb core for trunk loadfloors and applications to the automotive sector [15]. In the marine industry, some significant developments have been recently made, with the Gwalaz sailing boat made of bio-based sandwich materials (flax fibres, balsa wood and cork) being one of the prime examples [16]. Sandwich materials with flax fibre skins and agglomerated cork core have been also used by University of Palermo as a structural component for a sailing boat [17]. An example of civil/infrastructure application is the bio-based sandwich pedestrian bridge made of flax fibre composite skins and cork/PLA foam core deployed over the river Dommel in Eindhoven, Netherlands [18]. For

the latter application, the designers have however pointed out the uncertainty regarding the long-term behaviour (creep in particular), and the dependence of the stiffness and the strength versus temperature and moisture [19]. In civil engineering, bio-based sandwiches are used as building walls for sound insulation and temperature isolation. For this application, the impact and flexural behaviour of sandwich is highly inspected [20–24]. The majority of the bio-based composite sandwich materials and structures developed so far have been indeed tested under monotonic, dynamic, fatigue or impact loading conditions [20,25–37]. There is a certain lack of data and knowledge in open literature concerning the long-term behaviour, in particular creep bending under hygrothermal conditions. Chen *et al.* [38] have evaluated the 3-point bending creep behaviour of sandwich materials made of wood fibre composite skins, and the influence of the type of cardboard honeycomb core and its orientation on the viscoelastic properties of the structures. Tests have been realised at 21°C and 70% relative humidity (RH). The ribbon of the honeycomb was either oriented following the length of the sandwich beam, or perpendicular to the length of the beam itself. Those authors have shown a lower time-delayed deflection for sandwich panels with the direction of ribbon oriented along the beam's length. The corrugated paper honeycomb core also produced a lower deflection when compared to the expanded core case. Du *et al.* [39] have studied the creep behaviour of a sandwich composites with cotton fibre/epoxy skins and aramid honeycomb core conditioned at a temperature of 20°C and relative humidity values of 50 % and 65 %. A tertiary creep stage was observed between 7 to 15 days of creep when the sandwich panels were subjected to bending stresses between 20% and 40% of the stress at break at 65% RH. Chen et al. [40] have also simulated by using a 3D moisture-displacement finite element model the influence of constant and cyclic humidity and varying temperature on the bending creep behaviour of a sandwich panel made of wood composite skins and kraft honeycomb core. The creep behaviour of the sandwich panel appeared to be affected by both the frequency and the amplitude of the humidity cycle. Results also have shown that the cyclic humidity made the creep of the sandwich panel more sensitive to the temperature. Studies available in open literature therefore show some quite complex creep behaviour and the presence of thermo-hygro-mechanical coupling, which justify the need of more in-depth analyses for bio-sourced sandwich materials under development.

The present work, carried out within the framework of the European project SSUCHY (www.ssuchy.eu), aims to replace the sandwich material currently used to manufacture a car trunk load floor with a more environmentally friendly sandwich panel solution. The benchmark solution here is a two-components polyurethane system of a compressed moulded glass fibre-reinforced sandwich panel (Baypreg®) [41] used for a variety of automotive parts (door panels, sunshades, spare tire covers, load floors). The sandwich panels are subjected to creep loads under

various and varying hygrothermal conditions, in the case of load floors applications. It is therefore of primary importance to characterise and model the behaviour of the replacement biobased materials under this type of mechanical and environmental loading. For the skins, we have selected a newly developed woven hemp fabric reinforced GreenPoxy composite system [42]. The tensile monotonic and creep behaviour of this composite have already been characterised and analysed in a previous work [43]. For this automotive application and based on preliminary design works, the approach was to consider several core types. For each type of core, only one density was chosen which is the most appropriated to the specifications. So, three different materials have been considered as the core: a reconstituted balsa wood panel, a paper honeycomb and a recycled PET foam. Those core materials have been chosen for their sustainable characteristics (bio-based or recycled materials), and their lightweight and shear mechanical properties. The shear creep behaviour of those sustainable cores has been also previously studied [44]. In the present work, the creep/recovery bending behaviour of the composite sandwich materials is evaluated under two different hygrothermal environments: 23°C-50% RH and 70°C-65% RH. Those two environments are labelled EC1 and EC2, respectively. The experimental results are also compared with a finite element simulation. The environmental impacts associated with the production of the different sandwich materials are assessed using a LCA methodology, and results are compared to the benchmark fossil sandwich structure configuration. The results from the LCA analysis can also further contribute to the optimisation of the production process of the sandwich composite panels by minimising the material and energy consumption and by investigating the generation of waste and pathways to valorisation.

2. MATERIALS AND METHODS

2.1. Materials

2.1.1. Skin and core materials

The reinforcement used for the composite skins is a balanced woven fabric made of hemp roving with a surfacel weight of 369 g/m² (Linificio e Canapaficio Nazionale, Bergamo, IT). The pattern is a satin 6 effect diagram with a density of ~ 6.5 yarns/cm in each direction. The twist level of the roving is approximately 40 turns per meter. More details can be found in [45]. The epoxy system is the GreenPoxy 56 resin and SD 7561 hardener (Sicomin, FR). Three different cores have been selected for their shear mechanical properties and their low density [44]**.** The first one is an end-grain balsa wood panel Baltek SB50 from 3A Core, provided by Sicomin. This material is in the form of a rigid panel, with a thickness of 25.4 mm, made of balsa blocks assembled by a polyvinyl acetate

adhesive bonding. The length and the width of the panel is labelled as L and T material directions, respectively. A 8 cell size paper honeycomb H-3D-140-1400-8.1-20.0-N-57 (Axxor, NL) with a thickness of 20 mm has been chosen as second core material. The chosen direction of the ribbon is the L-one. The last core considered in this work is a recycled polyethylene terephthalate (rPET) foam ArmaPET Struct GR80, with a thickness of 20 mm (Armacell, BE). The panel of rPET has darker colour lines that correspond to the welding lines. The L-direction is considered parallel to those lines.

2.1.2. Sandwich structure

The sandwich panels have been produced in two steps. The first consists in the production of the composite skins; the second involved the bonding of those skins to the core materials.

Composite skins manufacturing

The skins have been manufactured using an Agila 100kN thermocompression machine. The reinforcement plies are cut following the dimensions of a 300x200 mm² steel mould previously covered with Teflon. Before stacking, the plies have been dried at 60 °C for 24 h at least. Only one ply per skin has been used. Each ply is impregnated by hand with the epoxy system. The two skins have been manufactured in one step using a two-levels mould, to guarantee the same fabrication conditions for each of them. The mould was then put in the thermocompression machine. The temperature of the mould was measured using a thermocouple. A pressure of 3 bars is applied to the mould once the temperature reaches 40°C. After 15 mins, the temperature has been set to 60°C. Once this temperature is reached, a one-hour delay follows, after which, the heating is stopped. The pressure has been released when the temperature of the skin is close to 35°C. The mean (average) thickness of the composite skins is about 0.53 mm and the fibre volume fraction is approximately 0.43, following a measurement procedure detailed in [43].

Skins/core bonding

To have an identical value in all the sandwich panels, the thickness of the balsa wood core is first reduced to reach a value of 20 mm by using a grading machine Jet 16-32 Plus. The cores are then stored in a room where the temperature and the relative humidity are at 23±3°C and 50±10% RH, respectively. The skin and the core materials have then been bonded. A foaming epoxy system (PB170 and D02), provided by Sicomin, is used to improve the skin/core bonding, in particular for the open cell cores. A mass of 10 g of foaming epoxy has been applied on the surface of each skin using a spatula for a homogeneous repartition of the adhesive. The skins are oriented so that

the weft direction corresponds to the length of the sandwich plates. The L-direction of the balsa wood panel and the paper honeycomb and the T-direction of the rPET foam also correspond to the direction of the length of the sandwich plates. Skins and core are then assembled in the mould and put into the thermocompression machine. A pressure of 0.2 bar is applied, in a range of time between 1 and 3 seconds, to the sandwich panel, and then the temperature increased until reaching 130°C. After one hour, the pressure is released and the heating plates switched off.

2.1.3. Sandwich panels samples and conditioning

After manufacturing, the sandwich plates have been stored in a Memmert HPP 108L climatic chamber under the hygrothermal conditions EC1, corresponding to 23 °C-50 % RH. The sandwich panels have then been cut into beams using a thin-cutting band saw. The samples are then separated into two batches, conditioned for at least 20 days in the EC1 and EC2 (70 ±3 °C-65±5 % RH) environments, respectively. The durations of the conditioning have been chosen following preliminary tests to ensure that the equilibrium moisture content is reached, i.e., when an infinitesimal mass change is measured between two measuring times. The dimensions of the different samples used for the mechanical tests are approximately 280x40x21 mm^3. Small variations in thickness have been caused by the conditioning in the EC2 environment. The exact dimensions of the samples are listed in the supplementary data. Sandwich materials are labelled differently, according to the core type: SHB, SHN and SHP are related to the balsa wood, paper honeycomb and rPET foam cores, respectively. The Table 1 presents the type of mechanical test, the environmental condition of the test and the number of samples tested.

Table 1. Number of sample and dimensions of the sandwich as a function of the core type, the mechanical test and the environmental test condition

Sandwich	Core	Test	Environmental condition	Dimensions (length x width x thickness)	Number of samples
SHB	Balsa wood	Monotonic	EC1	280x40x21.60	4
			EC2	280x40x21.39	4
		Creep/recovery	EC1	280x40x21.16	3
			EC2	280x40x21.40	3
SHN		Monotonic	EC1	280x40x20.83	3

	Paper Honeycomb		EC2	280x40x20.95	3
		Creep/recovery	EC1	280x40x20.86	3
			EC2	280x40x20.88	3
SHP	rPET foam	Monotonic	EC1	280x40x21.17	4
			EC2	280x40x21.22	4
		Creep/recovery	EC1	280x40x21.11	3
			EC2	280x40x21.25	3

2.2. Mechanical testing

2.2.1. Monotonic bending tests

The behaviour of the sandwich beams is evaluated in a 4-points bending rig with a 200 mm length between the supports. The loading span is equal to 100mm. An MTS Criterion 45 tensile machine with a 5 kN cell load has been used, with a displacement rate of 1 $mm.s^{-1}$. The diameter of the pins is 10 mm.

The average value of temperature and relative humidity in the test room during the test performed in the EC1 environment has been measured at 23±3 °C and 50±10 % RH, respectively. A laser displacement sensor OptoNCDT with a 10 mm stroke is used to measure the displacement of the sandwich at the mid-span, labelled as W. The tests have been stopped after the failure of the specimen.

Tests in the EC2 environment have been performed with an in-house chamber made of polymethyl methacrylate (PMMA) and connected to a humidity generator Inec 70/90 installed on the tensile machine. The deflection at the midspan is measured using a LVDT sensor with a stroke of 10 mm. Figure 1 shows the test bench. The tests have been stopped when reaching a deflection of 8.5 mm, if failure was not occurring before.

The bending stiffness of the sandwich beam is calculated as the ratio between the load P and the mid-span deflection W. The influence on the bending stiffness caused by the small variations in thickness observed in the EC2 environment is estimated using sandwich beam theory [1]. The results show that the geometry deviations cause a maximum variation in stiffness of approximately 5 %. The P/W bending stiffness has therefore been deemed as sufficient to compare the performance the different sandwich panels tested in the two different environments.

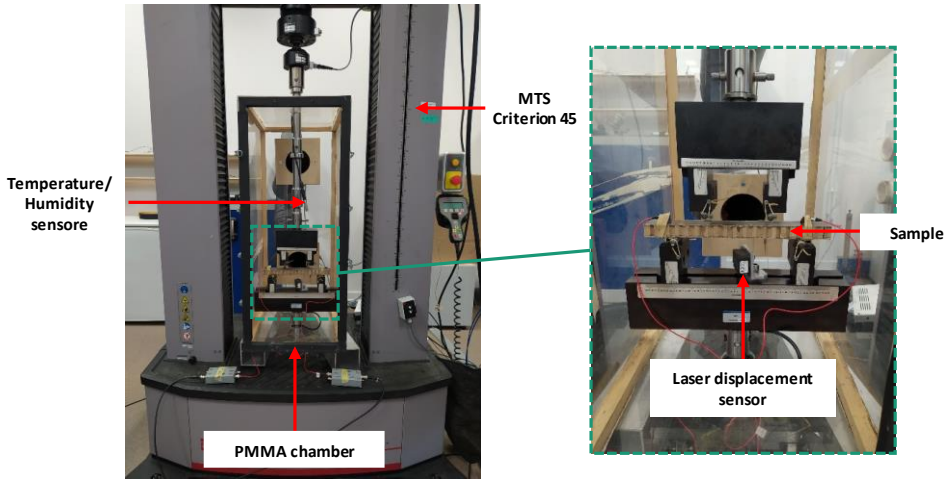

Figure 1. Pictures of the testing machine and of the bending test bench installed in the climatic chamber connected to the relative humidity generator

2.2.2. Creep bending tests

The time-delayed behaviour of the sandwich beams is also evaluated using a 4-point bending test with a 200 mm length between supports. The loading span is equal to 100mm. The tests have been performed using the same machine and configuration as for the monotonic bending tests. The load path is divided into one hour of creep and one hour of recovery. The nominal load has been reached after 2 seconds. All the tests have been performed under load control. A 3 MPa stress has been applied on the sandwich beams made of balsa wood. The stress applied to the other sandwich beams is 1.5 MPa. All these values correspond to approximately 1/3 of the ultimate bending stress. The bending stress in the sandwich beam considered as a homogenous material is calculated as follows:

$$\sigma_{bend} = \frac{3F_{nom}L}{4bh^2} \quad (1)$$

In (1), F_{nom} is the nominal force; L is the span length; b and h are the width and the thickness of the sandwich beam, respectively.

The following parameters have been identified from the raw experimental data:

- the instantaneous deflection W_{ins}^{c} corresponding to the value of the total deflection once the nominal force F_{nom} is reached for the first time. This parameter takes also into account the displacement occurring during the run of the test.

- the instantaneous stiffness $\frac{P}{W_{ins}}$ is determined within a force range between 75 N and 150 N.
- the maximum deflection W_{max} is determined during the creep/recovery test.
- the time-delayed strains W_{del}^{c} and W_{del}^{r} are determined during the creep and the recovery stages, respectively.
- the instantaneous deflection is determined during the unload W_{ins}^{r}, corresponding to the difference between W_{max} and the value of the total deflection at the beginning of the recovery stage.
- the deflection rate $\dot{W}_{creep}$ is determined within a timescale between 2000 s and 3500 s.
- the residual deflection determined at the end of the recovery stage W_{res}.

All those parameters are illustrated in Figure 2. The latter shows a typical creep/recovery response in load/deflection, and the deflection time histories.

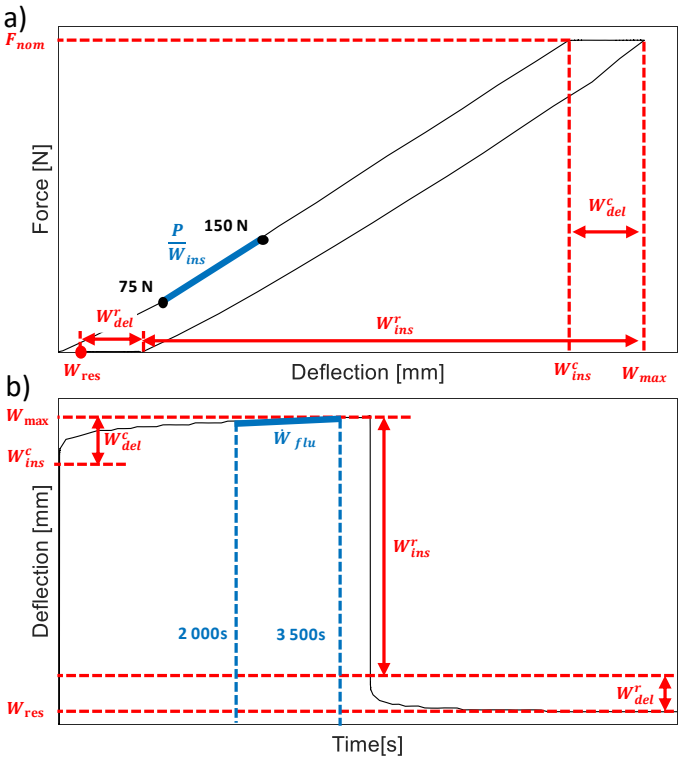

Figure 2. Mechanical parameters identified from the force-deflection a) and deflection-time b) diagrams

2.3. Finite element simulation

The creep flexural behaviour of the sandwiches has been simulated using 3D finite element analysis for the two environmental conditions EC1 and EC2. Although the structure is very thin, shell elements have not been kept because of the particularities of the sandwich behaviour regarding to the shearing effect. The dimensions of the sandwiches are those described in the Table 1 for creep/recovery tests. The composite and the core were modelized as a homogeneous material. The skin and the core were considered as elasto-viscoelastic materials. The viscoelastic model is the one presented in our previous papers [43,44] and the material properties, used in this model, are those already identified at composite and core scales. However, the viscoelastic properties depend on the stress level and the stress level in the sandwich components, determined with sandwich theory, doesn't correspond with the ones studied at composite and core scales. The value of the viscoelastic properties were so taken for a stress being the much closer to the stress, calculated with the sandwich theory, in the component. These values are also resumed in the supplementary data section. The 4-points flexural test was modelized by a simple support at the extremities of the sandwich. The load was assumed to be a force applied on a nodes line along the sandwich width (Cf. Figure 3).

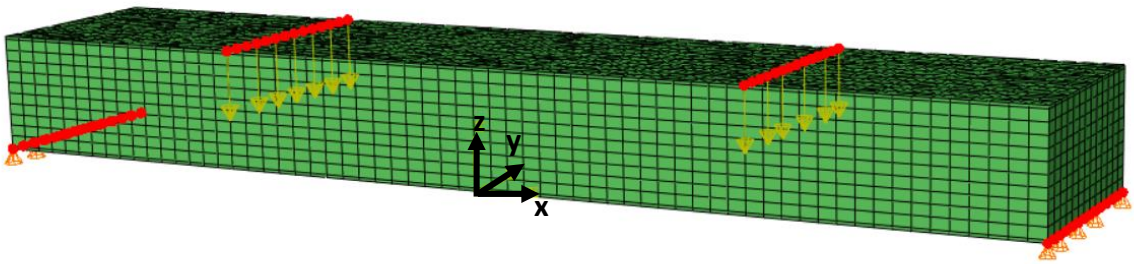

Figure 3. Meshed model of sandwich and boundary conditions

The mesh is first realized in the (x,y) plane using GMSH software. A node was imposed to be in the middle of the sandwich following the width and the length. The strain values were so taken in this point to correspond to the measure realized during experimental test. The 2D mesh was then extruded. In the normal direction, there are 10 elements in the core thickness and one in the skin thickness. The meshed model was made of approximately 11 500 nodes and 18 800 elements. The finite element solver ABAQUS was used. The CPU time was around 10 600 seconds.

2.4. LCA of different sandwich panels

LCA has been performed to assess the environmental performance of the different sandwich panel solutions [46,47]. This LCA study aimed to provide and compare the global warming potential (GWP) including biogenic carbon for the different combinations of the sandwich panels: hemp-Greenpoxy composite skins and the benchmark of polyurethane-glass fibre composite skins. The scope of the study is cradle-to-gate, which includes the procurement, transport, and manufacturing steps of the sandwich panels. These materials being in a development step, the LCA study focuses only on the manufacturing step to distinguish the impacts related to the production and the other one related to the use phase. The process flow diagram of the scope of this study is provided in Figure 4. The functional unit for this study is the specific bending stiffness, calculated by dividing the bending stiffness by the apparent density of the sandwich panels. Regarding the sandwich structures with hemp fibres-based skins, the values used have been issued from experimental measurements. The bending stiffness values of the sandwich panels with glass fibres-based skins were calculated using the sandwich beam theory. The elastic properties of the skins have been extracted from the work by Cageao *et al.* [41] and correspond to 1.2 mm thick skins made of a glass mat with a surface weight of 900 g/m² (per skin) and PU resin (with a mass fraction of 50%). The sandwich beams thickness for this benchmark solution is also 20 mm. The values of the shear modulus and density of the core materials used for the calculation were extracted from [44]. The core and skin were considered perfectly bonded. The values of the apparent density, the bending stiffness and the specific bending stiffness for the different materials are given in the Table 2.

As a result, for each specific panel, the mass and energy balances have been extrapolated according to the amount in kg of the sandwich panel, which provides a specific bending rigidity of 1 $kN.m^2.kg^{-1}$. The mass and energy balances for the sandwich panels correspond to the inventory data provided by the SSUCHY project partners. As previously mentioned, the three main sandwich panels include the hemp and glass fibre-based composite skins, and 3 core possibilities: paper honeycomb, balsa wood, and rPET foam. Based on the inventory, the LCA models were created on the GaBi software, using the Ecoinvent 3.3 and ThinkSteps databases. For all processes, the European market group data was used wherever applicable. If the data does not exist, the global market average was used. The electricity grid mix data was assumed to be the French electricity grid mix.

Figure 4. Process flow diagram of the production of the bio-based sandwich composite panel

The data related to the reinforcements of the bio-based sandwich panels have been sourced from SSUCHY project partners. Throughout the manufacturing steps, the mould is assumed to be reused. The hardener has been assumed to be ethylenediamine, according to Gan *et al*. [48] and Three Bond Co., Ltd. [49]. The corrugated cardboard box production layout of Ecoinvent 3.3 [50] has been assumed to represent the one of the paper honeycomb cores. To represent production of the balsa wood core, the market for sawn wood, board, hardwood, dried, planed from Ecoinvent 3.3 has been used. The balsa wood plane board has been assumed to be produced in Ecuador, the world's top producer [51], and shipped by freight ship transport (the market for transport, freight, sea, transoceanic ship) from the port of Guayaquil, Ecuador to the port of Le Havre, France with the total distance of 13740 km. Subsequently, the balsa wood boards have been then transported via truck lorry transport (market for transport, freight, lorry 16-32 metric ton, EURO4) from the port of Le Havre to the city of Besançon, France for 610 km. The GWP data from Armacell has been used as an indicative value for the GWP of the rPET foam production, according to Armacell [52]. The productions of the rPET foam core and the paper honeycomb have been assumed to have occurred in Besançon, France. Polyurethane adhesive foam is used as the adhesive foam for the bonding of the skins in the LCA models. The glass-fiber-reinforced polyurethane benchmark composite has been modelled following the production protocol described by La Rosa *et al.* [10]. The ReCiPe midpoint 2016 (H) has been used for the life cycle impact assessment methodology. The climate change, including biogenic carbon, impact category results in kg. of carbon dioxide equivalents are reported within this study. In addition to this, the sensitivity analysis of the input parameters was conducted. Firstly, the contribution of each process parameters on the GWP was analysed in order to identify and illustrate the impacts distribution and hotspots of the hemp-based skins production. Consequently, the identified parameters are analysed in a sensitivity analysis to illustrate the variations in the GWP when all the input parameters are decreased or increased by 10%.

Table 2. Comparison of the specific bending rigidity and the mass reference flow of bio-based sandwich panels made of hemp fibres-based skins, and of the benchmark sandwich panels with glass fibre-reinforced skins.

Types of sandwich panel (fibre reinforcement/matrix/core)	Apparent density [$kg.m^{-3}$]	Bending stiffness (P/W)	Specific bending stiffness	Amount of material to obtained same

		[N.mm^{-1}]	[kN.m^2.kg^{-1}]	bending stiffness [kg]
Hemp fibre/ GreenPoxy/Balsa wood	168	452	2.7	0.37
Hemp fibre/ GreenPoxy/ Paper honeycomb	127	360	2.8	0.35
Hemp fibre/ GreenPoxy/ rPET foam	156	261	1.7	0.58
Glass fibre/ Polyurethane /Balsa wood/	265	759	2.9	0.34
Glass fibre/ Polyurethane /Paper honeycomb	221	589	2.7	0.37
Glass fibre/ Polyurethane/rPET Foam	250	370	1.5	0.66

3. RESULTS AND DISCUSSION

3.1. Monotonic bending behaviour under hygrothermal conditions

The Figure 5 presents the bending force/deflection curves of the SHB, SHN and SHP beams tested in the EC1 and EC2 environments. The values of the bending stiffness and the maximum load for these two environments are given in Figure 6.

Under the EC1environment, the bending behaviour of all the materials of the sandwich structures is linear until a yield point, after which the curve becomes nonlinear. The bending stiffness of the SHB sandwich beam is the highest, with a value of 452 N.mm^{-1}. The mass of that sandwich beam is however higher than the one of the other two, that's why the specific bending stiffness was also considered. The values of this parameter are equal to 2.7, 2.8 and 1.7 kN.m^2.kg^{-1} for the SHB, SHN and SHP structures, respectively (see Table 1). The SHB and SHN sandwich structures are the ones that perform the best in terms of specific bending stiffness. The SHB also presents the highest maximum force with a mean value of 1403 N, against the 468 N and 498 N for the SHN and SHP cases, respectively.

Under the EC2environment, the bending behaviour is still linear until a yield point, and then becomes nonlinear. For the SHP material, the shape of the nonlinearity differs from the one observed during testing in the EC1 environment. This is due to a significant indentation of the sandwich under the loading points. For the SHB, SHN and SHP cases, the bending stiffness at EC2 is 43 %, 56 % and 64 % lower when compared to EC1 environment.

The decrease of the sandwich stiffness with the increasing severity of the hygrothermal conditions is attributed to the decrease of the tensile modulus of the composite skins [43], and of the shear modulus of the core materials [44]. Moreover, it was observed that the decrease in terms of shear modulus is more important for the rPET foam core than for the balsa wood. The decrease of the bending properties of the sandwich beams could also be due to the cumulative microstructural damage at the skin/core interface; this was previously mentioned in open literature for other sandwich materials [28].

The strength of the sandwich panels is also affected by the severity of the hygrothermal conditions. The maximal force decreases by 51%, 42% for the SHN and SHP structures, respectively, when compared to the properties measured in the EC1 environment. No failure has been observed before the end of the test for the SHB structure. The preferential failure modes of the SHN and SHP sandwich panels are core/skin debonding and indentation, respectively. For the SHP case, the failure mode can be explained by the decrease of the compressive strength of the rPET foam core with the severity of the environment.

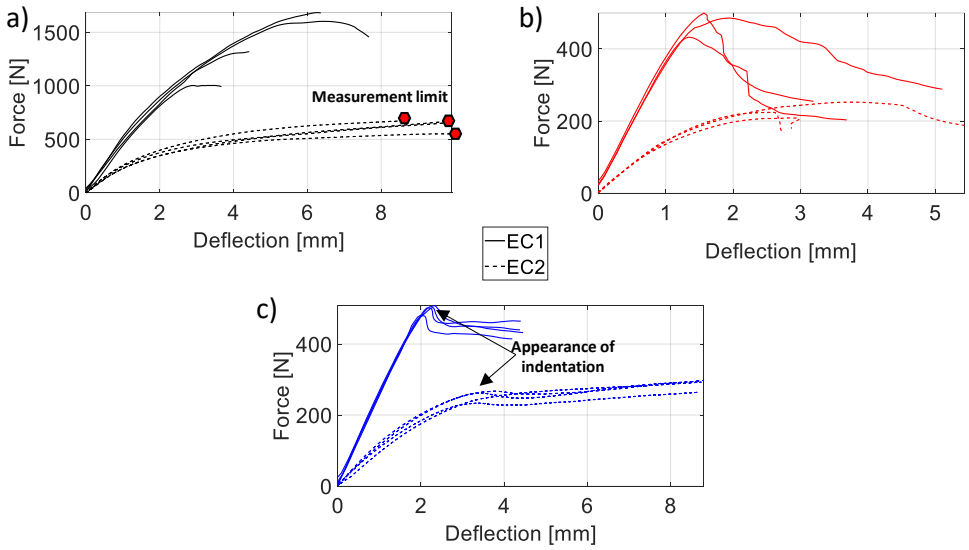

Figure 5. Bending behaviour of the sandwich panels SHB (balsa wood core) a), SHN ((paper honeycomb core) b) and SHP (recycled PET core) c) tested in the EC1 (23°C-50%RH) and EC2 (70°C-65%RH) environments

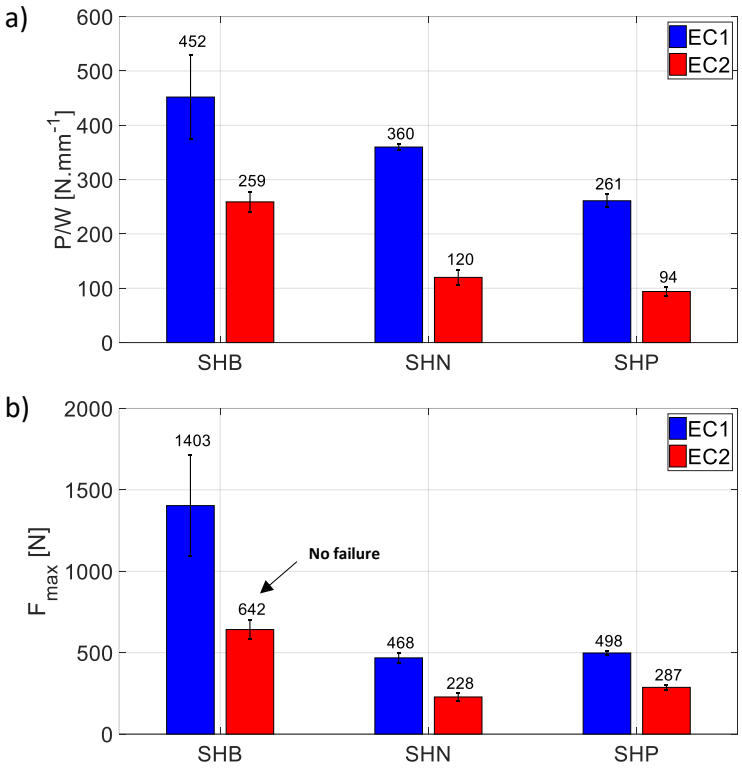

Figure 6. Values of stiffness a) and maximum force b) as a function of the type of sandwich structure (SHB: balsa wood core; SHN: paper honeycomb core; SHP: recycled PET core) and environment (EC1: 23°C-50%RH; EC2: 70°C-65%RH)

3.2. Creep/recovery bending behaviour under hygrothermal conditions

3.2.1. Environment EC1

The creep/recovery behaviour of the sandwiches under monotonic loading has been first evaluated in the EC1 environment. Figure 7 presents the time history of the deflection for the three cases of sandwich panels. Under loading, the deflection of the sandwich beam can be divided into an instantaneous part, and a time-delayed part. This second one is characterised by a primary and then a secondary creep phase. The deflection then decreases as the material is unloaded. The displacement evolves during recovery in a similar way to that observed during creep. The mechanical parameters identified from the creep/recovery tests are given in the Table 3. The values of the instantaneous bending stiffness ($\frac{P}{W_{ins}}$) are equal to 412 N.mm^{-1}, 432 N.mm^{-1} and 259 N.mm^{-1} for the SHB, SHN and SHP cases, respectively. These values agree with those obtained during the monotonic bending tests for the SHB and SHP beams. For the case of the SHN structure, the bending stiffness is 17% higher during the loading phase of the creep test, than during the monotonic test. This is explained by the dependence of the shear behaviour of the paper honeycomb on the deflection rate [44], which is 1 mm.min^{-1} during monotonic loading and approximately 1 mm.s^{-1} for creep/recovery tests.

Small residual displacements can be observed at the end of the recovery plateau. This was attributed to the presence of viscoelastic strains not fully recovered under the considered time scale, and to the small displacements induced by the positioning of the specimen at the beginning of the loading phase (i.e., rigid body movements and fitting clearance of the test rigs) before undergoing the real bending of the beam. It can be also observed that for all the materials, the amplitude of the delayed deflections measured during creep is similar to the one measured during the recovery phase.

To compare the performance of the different materials in terms of time-delayed properties, the viscoelastic compliance, defined as the ratio between the time-delayed deflection W_{del}^{c} and the bending stress, was calculated and is plotted in the Figure 8. The behaviour of all the sandwich panels in the EC1 environment is similar, the curves are superimposed.

3.2.2. Environment EC2

The mechanical parameters of the SHB, SHN and SHP structures identified in the EC2 environment are available in Table 3. The time history of the strain is shown in Figure 7. For all the SHP samples, the test is stopped in the creep phase, following the failure of the sandwich panels. This failure is mostly due to the high indentation level of the specimens (see Figure 9). For the SHB and SHN cases, the creep/recovery test is not interrupted by any failure, but the presence of damages is still observed after testing. Damage is mainly due to a combination of buckling of the upper skin (subjected to compression loading) and skin/core debonding (see Figure 9). Despite the occurrence of these macroscopic damages, no obvious change can be detected in the time-delayed deflection shown by the creep curves (whether within the primary or secondary creep phases). It is possible to observe a in the SHP beams a tertiary creep phase before failure, due to the indentation of the sandwich panel under the supports. These damage mechanisms appear on SHB, SHN and SHP for forces corresponding to 56%, 75%, 61% of the maximum bending force, respectively.

The values of the instantaneous stiffness of the SHB, SHN and SHP beams are 49%, 66% and 64% lower than the corresponding values measured within the EC1 environment. All these values agree with the monotonic properties measured within EC2. The results also show that the time-delayed deflection during the creep phase is larger than in the recovery phase. Furthermore, the residual deflections at the end of the tests are quite significant, with average values of 1.98 mm for the SHB and 0.83 mm for the SHN beam. These elements indicate the presence of

irreversible mechanisms occurring under loading, which contribute to the increase in deflection during creep. The presence of damages has been indeed observed at the sandwich beam scale after the creep/recovery tests (Figure 9). Internal stresses may also remain within the material and cause additional deflection. This behaviour observed at the sandwich beam scale may also be induced by the non-linear behaviour of the composite skins [43].

The evolution of the viscoelastic compliance is also shown in Figure 8 for tests realised in the EC2 environment. Compared to EC1, a significant increase (more than two decades) of the viscoelastic compliance is observed for all the materials considered. The related curves are still superimposed for the SHB and SHN structures, but not for the SHP case; the latter shows a larger deflection in the primary creep stage, and at the end of which a failure is observed. Contrary to the measurements in the EC1environment, the viscoelastic compliance at the end of the creep stage depends on the type of core, with values equal respectively to 0.97 $mm.MPa^{-1}$, 1.16 $mm.MPa^{-1}$ and 3.23 $mm.MPa^{1}$ for SHB, SHN and SHP structures, respectively. The time-delayed behaviour of the balsa wood core sandwich shows a lower shear deformation than that exhibited by the paper honeycomb and recycled PET foam core sandwich structures. Taking both environmental conditions into account, it appears that the sandwich structures with the balsa wood core perform best during the creep experiment.

Figure 10 compares the values of the residual deflections and the instantaneous and time-delayed deflections, measured during the creep phase for all the sandwich structures in both environments. For all the sandwich panels, the instantaneous deflection increases with the severity of the environment. this deflection increases from a value of 1.19 mm in the EC1 to 3.42 mm in EC2 for SHB, from 0.72 to 1.29 mm for SHN and from 1.02 to 2.71 mm for the SHP case. An increase of the time-delayed deflection measured during the creep phase is also observed. At the end of the creep plateau, this parameter reaches the values of 2.79 mm, 1.68 mm and 4.92 mm for the SHB, SHN and SHP, respectively. Moreover, it is noteworthy that the time-delayed deflection measured in the EC2 environment is of the same order of magnitude or even higher than the instantaneous deflection for all sandwich structures. Therefore, for a PFC structure subjected to a creep loading, the instantaneous deflection is not the only one parameter to consider in the design. The time-delayed behaviour of the sandwich material can lead to an additional deflection with amplitude, which can be larger than the instantaneous one and depends on the severity of the environment. These results point out to the necessity to developing a time dependency mechanical model for PFC structures.

Table 3. Value of the mechanical parameters identified from creep/recovery tests realized on the sandwich panels (SHB: balsa wood core; SHN: paper honeycomb core; SHP: recycled PET core) in the EC1 (23°C-50%RH) and EC2 (70°C-65%RH) environments

	SHB		SHN		SHP	
	EC1	EC2	EC1	EC2	EC1	EC2
$\dot{W}_{creep}.10^{-6}$ $[mm.s^{-1}]$	9.0±2.3	288±16	4.6±1.4	144±58	4.9±0.3	-
$\frac{P}{W}_{ins}$ $[N.mm^{-1}]$	412±8	210±2	432±62	149±17	259±10	94±3
W_{ins}^{c} $[mm]$	1.19±0.09	3.42±0.06	0.72±0.18	1.29±0.14	1.02±0.22	2.71±0.13
W_{ins}^{r} $[mm]$	0.72±0.07	2.38±0.18	0.45±0.04	1.46±0.23	0.77±0.03	-
W_{del}^{c} $[mm]$	0.12±0.002	2.91±0.08	0.06±0.01	1.74±0.49	0.06±0.004	4.98±0.17
W_{del}^{r} $[mm]$	0.14±0.01	1.97±0.32	0.06±0.007	0.74±0.11	0.07±0.04	-
W_{max} $[mm]$	1.31±0.09	6.33±0.06	0.78±0.18	3.03±0.61	1.07±0.22	7.69±0.09
W_{res} $[mm]$	0.45±0.13	1.98±0.09	0.26±0.13	0.83±0.28	0.23±0.17	-

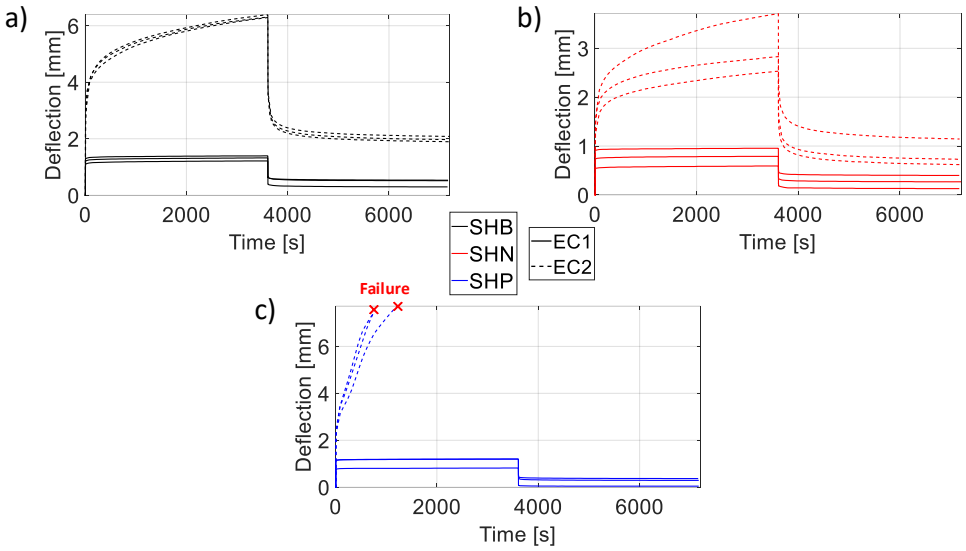

Figure 7. Bending creep/recovery behaviour of SHB (balsa wood core) a), SHN (paper honeycomb core) b), and SHP (recycled PET core) c) sandwiches tested in environment EC1 (23°C-50%RH) and EC2 (70°C-65%RH)

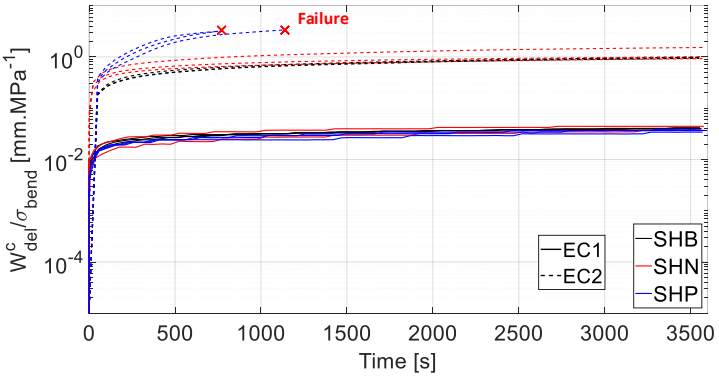

Figure 8. Evolution of viscoelastic compliance (defined as the time-delayed deflection normalized by the bending stress) of the sandwiches SHB, SHN and SHP (SHB: balsa wood core; SHN: paper honeycomb core; SHP: recycled PET core) tested in environment EC1 and EC2 (EC1: 23°C-50%RH; EC2: 70°C-65%RH)

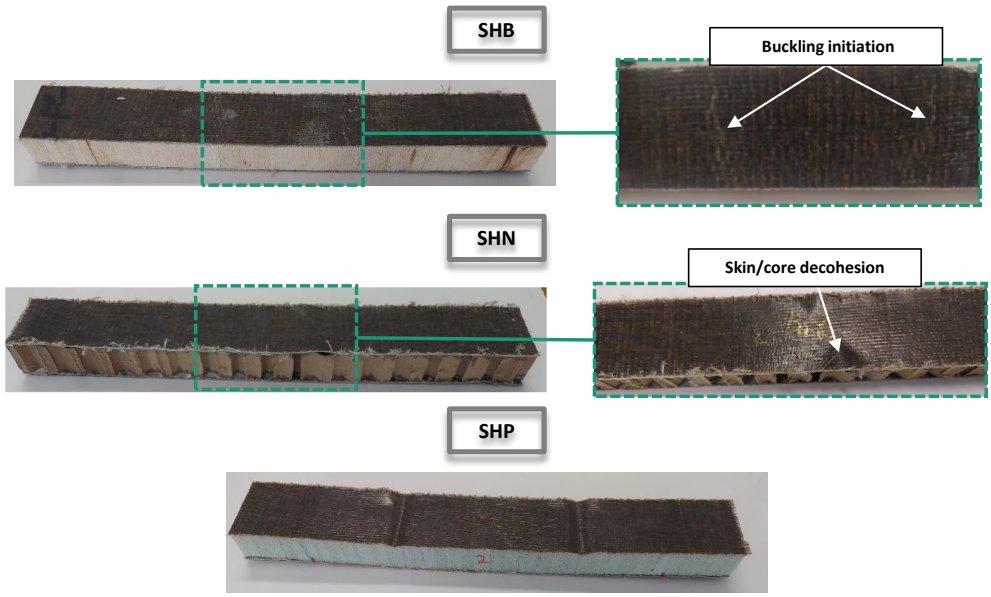

Figure 9. Damage mechanisms observed after creep/recovery tests in environment EC2 (70°C-65%RH)

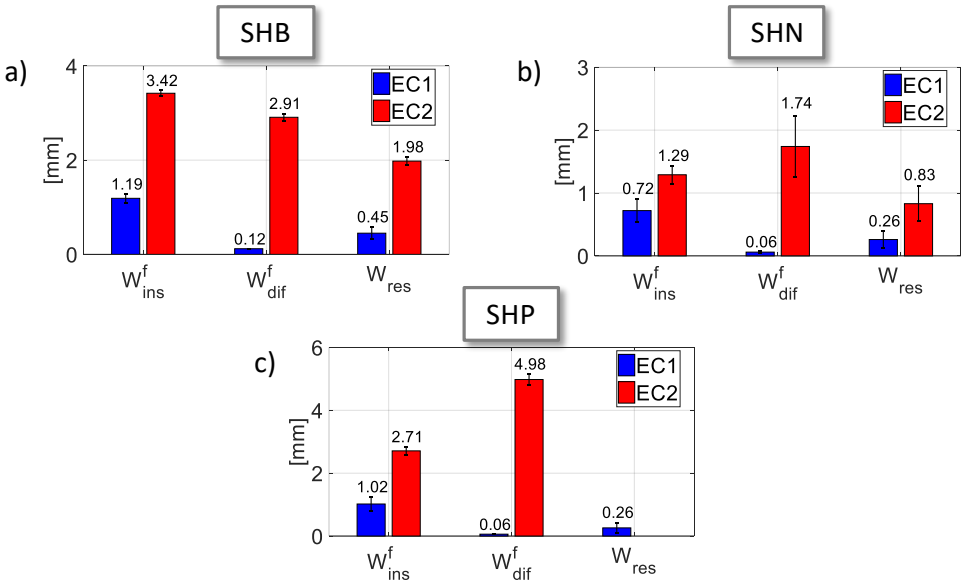

Figure 10. Values of instantaneous, time-delayed and residual deflection of SHB (balsa wood core) a), SHN (paper honeycomb core) b), and SHP (recycled PET core) c) sandwiches tested in environment EC1 (23°C-50%RH) and EC2 (70°C-65%RH)

3.3. Model/experiment comparison

The creep behaviour of the three studied sandwiches has been modelized using a finite element analysis. The experimental and modelled creep compliances of the sandwiches over time is compared in the Figure 11 for the two studied environmental conditions EC1 and EC2.

In environment EC1, the compliance obtained numerically at time 3600s are equal to $4.44.10^{-2}$ mm.MPa^{-1} for SHN and to $3.28.10^{-2}$ mm.MPa^{-1} for SHP. In comparison, the compliance measured experimentally is equal to 3.86. 10^{-2} mm.MPa^{-1} and to 3.66. 10^{-2} mm.MPa^{-1} for SHN and SHP, respectively. This difference corresponding to an error of 15% and 10% for SHN and SHB, respectively. Therefore, the identification of the viscoelastic at component scale allow to describe accurately the creep behaviour of the sandwich. Regarding the SHB sandwich, the model tends to minimize the deflection over time of the sandwich. A higher difference, around 60%, is noticeable between the compliance obtained with the finite element model and experimentally. The balsa wood core is considered in finite element analysis as homogeneous material. However, this material is made of assembled balsa block with different orientation and with a PVA adhesive. The hypothesis of a homogenous core material, when the sandwich is submitted to flexural solicitation, might be not realistic compared to what is observed experimentally.

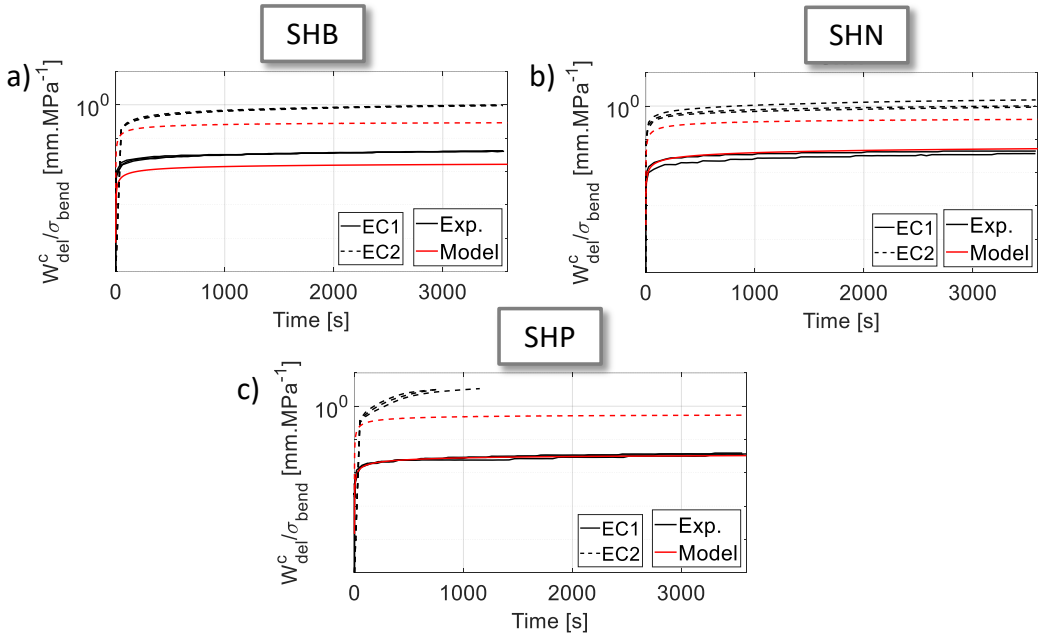

Figure 11. Comparison model/experiment of the creep compliance of the SHB sandwich (balsa wood core) a), the SHN sandwich (paper honeycomb core) b) and the SHP sandwich (rPET core) c) in environment EC1 (23°C-50%RH) and EC2 (70°C-65%RH)

In environment EC2, the limit of the viscoelastic model is observed. The compliance obtained experimentally is equal to 0.9675 mm.MPa^{-1}, 1.1572 mm.MPa^{-1}, 3.2339 mm.MPa^{-1} for SHB, SHN and SHP, respectively. Numerically, this parameter is 0.2887 mm.MPa^{-1}, 0.3973 mm.MPa^{-1}, 0.5382 mm.MPa^{-1},respectively. Instinctively, one can think that the compliance obtained with the model might be higher than the compliance obtained experimentally: the severe environment studied at composite scale being at 70°C-85%RH against 70°C-65%RH

at sandwich scale. However, the sandwich components are considered as viscoelastic without any irreversible or non-linear mechanisms. The presence of these latter was shown in latest paper [43,44] but no yet implemented in a finite element model. Moreover, these non-linearities have also been observed at composite and core scales under environment EC1 for higher stress levels. Based on these results and to design more accurately sandwich structures, there are a necessity to developed new model to consider the non-linear creep behaviour of sandwich structure in severe environment.

3.4. Assessment of the environmental impacts of the different sandwich materials

Figure 12 presents the results of the GWP for the production of the sandwich panels with a specific bending rigidity of 1 $kN.m^2.kg^{-1}$. The results are grouped according to the three core material options (paper honeycomb, balsa wood and rPET foam). For each group, the results for the hemp (blue bars) and glass (orange bars) fibre-based composite skins are represented. Across all groups, it is observed that the benchmark scenario with the glass-fiber-reinforced polyurethane shows in all scenarios a higher environmental impact than the hemp fibre reinforced composites. The reduction ranges from 29 to 40%, when the bio-based composites are compared with the petroleum-derived benchmark based on the different core types. It is noteworthy to mention that the overall trend for the GWP results of all the sandwich panels inversely reflects the trends of the specific bending stiffness, with the exception for the case of the balsa wood core. The results show that as the materials possess a higher specific stiffness, the GWPs decrease. This phenomenon is because when sandwich panels have higher specific stiffness, fewer materials, as well as energy, are consumed to develop sandwich structures with the same degree of specific stiffness. The LCA results also demonstrate that when the biogenic carbon is considered, the cases of paper honeycomb and balsa wood core feature lower GWP impacts than the rPET foam. This is because those core materials are bio-based. Therefore, additional avoided impacts for the GWP result from the use of bio-based core materials, in addition to the use of fiber reinforcements. This could explain the exception to the case of the balsa wood core, in which the GWP for the hemp-based solution is lower than the glass-based solution, despite having a lower specific stiffness. Since balsa wood is bio-based, carbon sequestration during the cultivation of the biomass and the conversion of the biogenic carbon within the carbon cycle of the composite production also contributes to the reduction in GWP. It is however important to mention that when other environmental impact categories are taken into account, the use of bio-based cores, particularly the balsa wood should be investigated more in detail, as they result in higher impacts related to agricultural activities [53]. Moreover, recent studies [51,54] have also pointed out the scarcity of the supply of balsa wood, which could drive additional future research for potential

alternatives. In order to further investigate the impacts of the input parameters for the hemp-based skins production, a local input parameter sensitivity analysis was performed. The effects of altering an input variable on the output are measured by LSA (one at a time). The main goal of LSA is to see how a minor perturbation around a reference input affects the final output result [55] (locally) the ranking of input parameters [56].

The results are illustrated in Figure 13. In essence, each input parameters of the hemp-based skins production were varied at a 10% variation. The corresponding changes in the GWP are then recorded and calculated into the sensitivity ratio. The results demonstrated that for all three hemp-based skins, the most impactful input parameter is the use of the epoxy resin in the skin production. Other input parameters that can influence the GWP include the use of the ethylenediamine, polyurethane foam and the hemp fibre reinforcement accordingly. The analysis showed that the remaining input parameters only have limited influence on the GWP. Furthermore, this trend can be observed for all three types of core for the hemp-based skins. To this end, the optimization of the required amount of these four components, particularly the epoxy resin, as well as the possibility to reuse or reduce the components could lead to further GWP reduction.

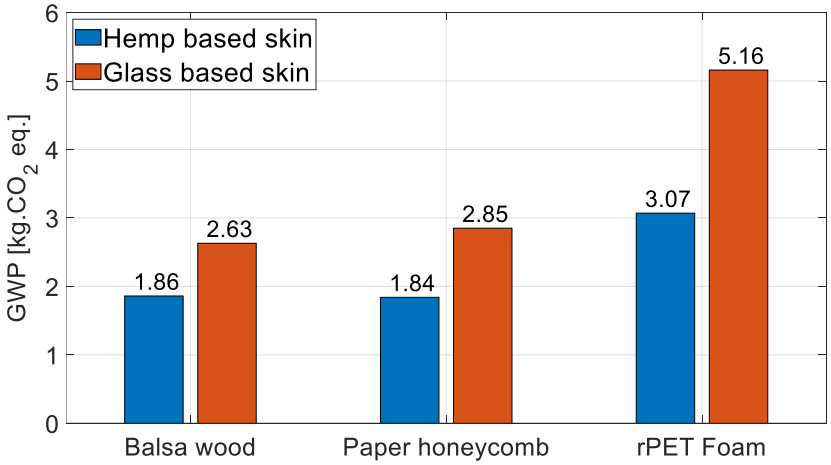

Figure 12. GWP production of panels with a specific rigidity of 1 kN.m².kg^{-1}.

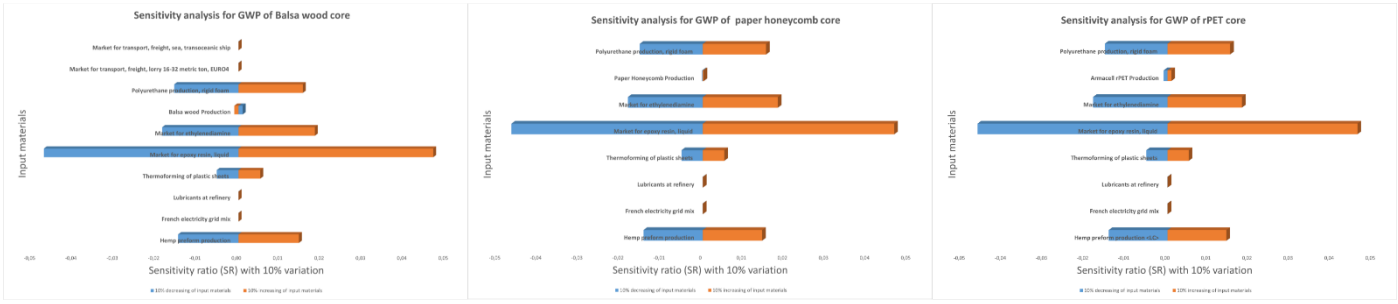

Figure 13: Sensitivity Analysis of the Input Parameters for the Hemp-based Skins Production

4. CONCLUSIONS

This study has presented the performance of the three classes of biobased sandwich materials in terms of environmental impact and creep behaviour under different hygrothermal conditions. The three sandwich panels materials are made of woven hemp fabric reinforced GreenPoxy composite skins and three different types of core materials (balsa wood panel, paper honeycomb and PET foam). The aim was to evaluate the possibility to replace glass fibre skin-based sandwich solutions with eco-friendly alternatives within an automotive application. The creep behaviour of sandwiches being a non-linear function of the density of the cores, the conclusions proposed in this paper must be restricted to the considered core materials' density.

The following points are highlighted:

- With respect to the environmental performance, the hemp fibre-reinforced composites perform better than the conventional glass-fibre-reinforced ones. The GWP is, in most cases, inversely proportional to the specific bending stiffness due to the fact that as the specific rigidity increases, there are less demands in terms of material and energy.
- In ambient conditions, hemp fibre-based sandwich panels with balsa wood and paper honeycomb core present the highest specific monotonic properties. The time-delayed compliance is similar for the thee sandwich types for the considered creep times. Noteworthy, both the monotonic bending stiffness and the strength decrease with the severity of the hygrothermal conditions.
- In EC2, after 1h of creep, the time-delayed deflection is of the same order of magnitude or even higher than the instantaneous response. So, it is of paramount importance to consider the time-delayed behaviour

in the design of such sandwich materials, in particular when they are exposed to quite severe hygrothermal conditions.

- Sandwich with rPET foam cannot resist to conditions as severe as the ones imposed in EC2, since tertiary creep induced by the foam shows collapse of the core material under the loading points.
- The simulated deflection at 23°C-50%RH shows a good correlation with the deflection obtained experimentally for sandwich with paper honeycomb and rPET foam. With the severity of the environment, the difference between the simulation and the experiment is larger and is attributed to non-linear mechanism not taking into account in the actual model.
- Considering the monotonic and creep performance in the two testing environments as well as the GWP, the balsa wood and the paper honeycomb-based sandwich beams appear to be the most relevant solutions to replace the conventional glass-fibre-reinforced composite sandwich structures.

This study was conducted only on the cradle-to-gate stage. The vehicle's mass increases fuel consumption which increases the CO_2 emissions [57]. It was discussed in this paper that the amount of material (mass) to achieve certain mechanical properties is 44% lower for the bio-based sandwich panels made of hemp fibre-based skins compared to the benchmark sandwich panels with glass fibre-reinforced skins. As a result of the above discussions, it can be concluded that when the bio-based sandwich panels are used in a vehicle, the mass of the vehicle will decrease and it will be expected to emit less CO_2 which means more environmentally friendly performance.

Considering the weight loss obtained with the bio-based sandwiches, a decrease of the environmental impacts during the use phase will expected. Indeed, it is well known that a slight difference in weight affects a lot the GWP related to the use phase of the car. To provide a comprehensive overview of the environmental performance of the bio-based composites, it will be also important to consider in the future other impact categories, in addition to the global warming potential.

Acknowledgements

The authors would like to acknowledge the funding received from the Bio Based Industries Joint Undertaking (JU) under the European Union's Horizon 2020 research and innovation program under grant agreement No 744349– SSUCHY project. The JU receives support from the European Union's Horizon 2020 research and innovation

programme and the Bio-based Industries Consortium. This work has also been supported by the EIPHI Graduate school (contract "ANR-17-EURE-0002"). The authors would also like to thank Linificio e Canapificio Nazionale for providing the hemp fabrics and Armacell Company for providing the rPET foam used in this study.

REFERENCES

[1] Zenkert D. The Handbook of Sandwich Structure. EMAS Publishing. 1997.

[2] Hellbratt S-E. Design and production of GRP sandwich vessels. Stockholm, Sweden: Dept. of Lightweight Structures, Royal Institute of Technology,; 1993.

[3] Seagrave TD. Automotive Polyurethane Composite Parts Made with Natural Fiber Mats and Honeycomb Cores n.d.

[4] Feng Y, Qiu H, Gao Y, Zheng H, Tan J. Creative design for sandwich structures: A review. Int J Adv Robot Syst 2020;17:172988142092132. https://doi.org/10.1177/1729881420921327.

[5] Binétruy C. Structures Sandwiches. Tech Ing 2008;TIB142DUO.

[6] Le Duigou A, Deux J-M, Davies P, Baley C. PLLA/Flax Mat/Balsa Bio-Sandwich—Environmental Impact and Simplified Life Cycle Analysis. Appl Compos Mater 2012;19:363–78. https://doi.org/10.1007/s10443-011-9201-3.

[7] Weiss M, Haufe J, Carus M, Brandão M, Bringezu S, Hermann B, et al. A Review of the Environmental Impacts of Biobased Materials. J Ind Ecol 2012;16:S169–81. https://doi.org/10.1111/j.1530-9290.2012.00468.x.

[8] Martin M, Røyne F, Ekvall T, Moberg Å. Life Cycle Sustainability Evaluations of Bio-based Value Chains: Reviewing the Indicators from A Swedish Perspective. Sustainability 2018;10:547. https://doi.org/10.3390/su10020547.

[9] Malviya RK, Singh RK, Purohit R, Sinha R. Natural fibre reinforced composite materials: Environmentally better life cycle assessment – A case study. Mater Today Proc 2020;26:3157–60. https://doi.org/10.1016/j.matpr.2020.02.651.

[10] La Rosa AD, Recca G, Summerscales J, Latteri A, Cozzo G, Cicala G. Bio-based versus traditional polymer composites. A life cycle assessment perspective. J Clean Prod 2014;74:135–44. https://doi.org/10.1016/j.jclepro.2014.03.017.

[11] Ghatak HR. Biorefineries from the perspective of sustainability: Feedstocks, products, and processes. Renew Sustain Energy Rev 2011;15:4042–52. https://doi.org/10.1016/j.rser.2011.07.034.

[12] Özdemir A, Önder A. An environmental life cycle comparison of various sandwich composite panels for railway passenger vehicle applications. Environ Sci Pollut Res 2020;27:45076–94. https://doi.org/10.1007/s11356-020-10352-8.

[13] Demertzi M, Silvestre JD, Durão V. Life cycle assessment of the production of composite sandwich panels for structural floor's rehabilitation. Eng Struct 2020;221:111060. https://doi.org/10.1016/j.engstruct.2020.111060.

[14] La Rosa AD, Cicala G. LCA of fibre-reinforced composites. Handb. Life Cycle Assess. LCA Text. Cloth., Elsevier; 2015, p. 301–23. https://doi.org/10.1016/B978-0-08-100169-1.00014-9.

[15] Faurecia. Faurecia Flaxpreg wins JEC Europe 2015 Innovation Award in the semi-products category 2015. https://www.faurecia.com/en/newsroom/faurecia-flaxpreg-wins-jec-europe-2015-innovation-award-semi-products-category.

[16] Curto M, Le Gall M, Catarino AI, Niu Z, Davies P, Everaert G, et al. Long-term durability and ecotoxicity of biocomposites in marine environments: a review. RSC Adv 2021;11:32917–41. https://doi.org/10.1039/D1RA03023J.

[17] Mancuso A, Pitarresi G, Tumino D. Mechanical behaviour of a green sandwich made of flax reinforced polymer facings and cork core. Procedia Eng 2015;109:144–53.

[18] Lepelaar M, Hoogendoorn A, Blok R, Teuffel P. Bio-Based Composite Pedestrian Bridge–Part 2: Materials and Production Process, Tokyo: 2016, p. 11.

[19] Blok R, Teuffel P. Bio-Based Composite Bridge – Lessons Learned. Proc IASS Annu Symp 2017 "Interfaces Archit Eng Sci 2017:9.

[20] Oliveira PR, May M, Panzera TH, Scarpa F, Hiermaier S. Improved sustainable sandwich panels based on bottle caps core. Compos Part B Eng 2020;199:108165. https://doi.org/10.1016/j.compositesb.2020.108165.

[21] McCracken A, Sadeghian P. Corrugated cardboard core sandwich beams with bio-based flax fiber composite skins. J Build Eng 2018;20:114–22. https://doi.org/10.1016/j.jobe.2018.07.009.

[22] Betts D, Sadeghian P, Fam A. Experiments and nonlinear analysis of the impact behaviour of sandwich panels constructed with flax fibre-reinforced polymer faces and foam cores. J Sandw Struct Mater 2021;23:3139–63. https://doi.org/10.1177/1099636220925073.

[23] Fu Y, Sadeghian P. Flexural and shear characteristics of bio-based sandwich beams made of hollow and foam-filled paper honeycomb cores and flax fiber composite skins. Thin-Walled Struct 2020;153:106834. https://doi.org/10.1016/j.tws.2020.106834.

[24] Betts D, Sadeghian P, Fam A. Post-impact residual strength and resilience of sandwich panels with natural fiber composite faces. J Build Eng 2021;38:102184. https://doi.org/10.1016/j.jobe.2021.102184.

[25] Monti A. Élaboration et caractérisation d'une structure composite sandwiche à base de constituants naturels. Université du Maine, 2015.

[26] Sergi C, Boria S, Sarasini F, Russo P, Vitiello L, Barbero E, et al. Experimental and finite element analysis of the impact response of agglomerated cork and its intraply hybrid flax/basalt sandwich structures. Compos Struct 2021;272:114210. https://doi.org/10.1016/j.compstruct.2021.114210.

[27] Ávila de Oliveira L, Coura GLC, PassaiaTonatto ML, Panzera TH, Placet V, Scarpa F. A novel sandwich panel made of prepreg flax skins and bamboo core. Compos Part C Open Access 2020;3:100048. https://doi.org/10.1016/j.jcomc.2020.100048.

[28] Abakar M. Analyse des mécanismes d'endommagement et du comportement vibratoire d'un composite à constituants naturels dans un environnement hydrique. Université du Maine, 2019.

[29] Sarasini F, Tirillò J, Lampani L, Valente T, Gaudenzi P, Scarponi C. Dynamic Response of Green Sandwich Structures. Procedia Eng 2016;167:237–44.

[30] Pandita SD, Yuan X, Manan MA, Lau CH, Subramanian AS, Wei J. Evaluation of jute/glass hybrid composite sandwich: Water resistance, impact properties and life cycle assessment. J Reinf Plast Compos 2014;33:14–25. https://doi.org/10.1177/0731684413505349.

[31] Hoto R, Furundarena G, Torres JP, Muñoz E, Andrés J, García JA. Flexural behavior and water absorption of asymmetrical sandwich composites from natural fibers and cork agglomerate core. Mater Lett 2014;127:48–52. https://doi.org/10.1016/j.matlet.2014.04.088.

[32] Karaduman Y, Onal L. Flexural behavior of commingled jute/polypropylene nonwoven fabric reinforced sandwich composites. Compos Part B Eng 2016;93:12–25. https://doi.org/10.1016/j.compositesb.2016.02.055.

[33] Mak K, Fam A, ASCE M, Colin M. Flexural Behavior of Sandwich Panels with Bio-FRP Skins Made of Flax Fibers and Epoxidized Pine-Oil Resin. J Compos Constr 2015;19:1943–5614.

[34] Du Y, Yan N, Kortschot MT. Light-weight honeycomb core sandwich panels containing biofiber-reinforced thermoset polymer composite skins: Fabrication and evaluation. Compos Part B Eng 2012;43:2875–82. https://doi.org/10.1016/j.compositesb.2012.04.052.

[35] Stocchi A. Manufacturing and testing of a sandwich panel honeycomb core reinforced with natural-fiber fabrics. Mater Des 2014:10.

[36] Du Y, Yan N, Kortschot MT. Novel lightweight sandwich-structured bio-fiber-reinforced poly(lactic acid) composites. J Mater Sci 2014;49:2018–26. https://doi.org/10.1007/s10853-013-7889-1.

[37] Essid S. Sandwiches à fibres de lin et anas de lin: optimisation structure-imprégnation-propriétés. Université le Havre Normandie, 2020.

[38] Chen Z, Yan N, Deng J, Smith G. Flexural creep behavior of sandwich panels containing Kraft paper honeycomb core and wood composite skins. Mater Sci Eng A 2011;528:5621–6. https://doi.org/10.1016/j.msea.2011.03.092.

[39] Du Y, Yan N, Kortschot MT. An experimental study of creep behavior of lightweight natural fiber-reinforced polymer composite/honeycomb core sandwich panels. Compos Struct 2013;106:160–6. https://doi.org/10.1016/j.compstruct.2013.06.007.

[40] Chen Z, Yan N, Deng J, Semple KE, Sam-Brew S, Smith GD. Influence of environmental humidity and temperature on the creep behavior of sandwich panel. Int J Mech Sci 2017;134:216–23. https://doi.org/10.1016/j.ijmecsci.2017.10.013.

[41] Cageao RA, Lorenzo JM, Franken K. Studies of Composites Made with Baypreg® F: Component Selection for Optimal Mechanical Properties. Bayer Mater Sci 2004:7.

[42] Corbin A-C, Soulat D, Ferreira M, Labanieh A-R, Gabrion X, Malécot P, et al. Towards hemp fabrics for high-performance composites: Influence of weave pattern and features. Compos Part B Eng 2020;181:107582. https://doi.org/10.1016/j.compositesb.2019.107582.

[43] Sala B, Gabrion X, Trivaudey F, Guicheret-Retel V, Placet V. Influence of the stress level and hygrothermal conditions on the creep/recovery behaviour of high-grade flax and hemp fibre reinforced GreenPoxy matrix composites. Compos Part Appl Sci Manuf 2021;141:106204. https://doi.org/10.1016/j.compositesa.2020.106204.

[44] Sala B, Gabrion X, Jeannin T, Trivaudey F, Guicheret-Retel V, Scarpa F, et al. Effect of hygrothermal ageing on the shear creep behaviour of eco-friendly sandwich cores. Compos Part B Eng 2021:109572. https://doi.org/10.1016/j.compositesb.2021.109572.

[45] Corbin A-C. Développement et analyse multi-échelle de renforts en chanvre pour applications biocomposites. Université Lille Nord-de-France, n.d.

[46] European Commission, Joint Research Centre. ILCD handbook: general guide for life cycle assessment : detailed guidance. Luxembourg: Publications Office of the European Union; 2010.

[47] ISO 14040:2006. Environmental management – Life cycle assessment – Principles and framework. ISO - International Organization for Standardization; 2006.

[48] Gan J, Rosenthal C, Eckert MM, Kainz B, Trottier EC. Epoxy resin hardener compositions and epoxy resin compositions containing such hardener compositions. US8927663B2, 2009.

[49] ThreeBond. Curing agents for epoxy resin. Technical News; 1990.

[50] Wernet G, Bauer C, Steubing B, Reinhard J, Moreno-Ruiz E, Weidema B. The ecoinvent database version 3 (part I): overview and methodology. Int J Life Cycle Assess 2016;21:1218–30. https://doi.org/10.1007/s11367-016-1087-8.

[51] Cañadas-López Á, Rade-Loor D, Siegmund-Schultze M, Moreira-Muñoz G, Vargas-Hernández JJ, Wehenkel C. Growth and Yield Models for Balsa Wood Plantations in the Coastal Lowlands of Ecuador. Forests 2019;10:733. https://doi.org/10.3390/f10090733.

[52] Armacell. Life Cycle Assessment: PET foams. 2018.

[53] Nessi S, Bulgheroni C, Konti A, Tonini D, Pant R. Environmental sustainability assessment comparing through the means of lifecycle assessment the potential environmental impacts of the use of alternative feedstock (biomass, recycled plastics, CO2) for plastic articles in comparison to using current feedstock (oil and gas). JRC Technical reports; 2018.

[54] ACIAR. Balsa: biology, production and economics in Papua New Guinea. Australian Centre for International Agricultural Research Technical Reports 73; 2010.

[55] Groen EA. An uncertain climate : the value of uncertainty and sensitivity analysis in environmental impact assessment of food. Wageningen University, 2016. https://doi.org/10.18174/375497.

[56] Groen EA, Bokkers EAM, Heijungs R, de Boer IJM. Methods for global sensitivity analysis in life cycle assessment. Int J Life Cycle Assess 2017;22:1125–37. https://doi.org/10.1007/s11367-016-1217-3.

[57] Fontaras G, Zacharof N-G, Ciuffo B. Fuel consumption and CO 2 emissions from passenger cars in Europe – Laboratory versus real-world emissions. Prog Energy Combust Sci 2017;60:97–131. https://doi.org/10.1016/j.pecs.2016.12.004.

Supplementary Data

The values of the parameters used in the finite element analysis are given in the following table. The viscoelastic properties not given in the table are considered to be null.

Properties	Environment	Skin	Balsa wood	Paper honeycomb	rPET
E_x	EC1	16663	1	1	1
	EC2	5000	1	1	1
E_y	EC1	16663	1	1	1
	EC2	5000	1	1	1
E_z	EC1	4000	1146	130	57
	EC2	4000	1146	130	57
ν_{xy}	EC1	0.12	0.4	0.4	0.4
	EC2	0.12	0.4	0.4	0.4
ν_{xz}	EC1	0.25	0.4	0.4	0.4
	EC2	0.25	0.4	0.4	0.4
ν_{yz}	EC1	0.25	0.4	0.4	0.4
	EC2	0.25	0.4	0.4	0.4
G_{xy}	EC1	3000	123	49	19
	EC2	3000	88	31	
G_{xz}	EC1	1600	81	13	18

	EC2	1600	51	7	
G_{yz}	EC1	3000	1	1	1
	EC2	3000	1	1	1
τ_1	EC1	221.4	44	442413	270
	EC2	99.5	270	40135	73.7
SD	EC1	3.0	2.9	6.0	1.9
	EC2	2.8	4.0	5.3	2.73
β_x	EC1	0.11	0	0	0
	EC2	0.60	0	0	0
γ_{xz}	EC1	0	0.07	2.4	0.06
	EC2	0	0.38	3.18	3.48